Desalination and Water Treatment
www.deswater.com

1944-3994/1944-3986 © 2012 Desalination Publications. All rights reserved
doi: 10.1080/19443994.2012.708210

49 (2012) 130–135
November

Study of carbon aerogel-activated carbon composite electrodes for capacitive deionization application

D.K. Kohli*, Rashmi Singh, M.K. Singh, Ashish Singh, R.K. Khardekar, P. Ram Sankar, Pragya Tiwari, P.K. Gupta

Target Laboratory, Laser Materials Development and Devices Division, Raja Ramanna Centre for Advanced Technology, Indore 452 013, India
Email: kohli.devendra@gmail.com

Received 22 September 2011; Accepted 30 May 2012

ABSTRACT

Electrodes synthesized using mesoporous carbon aerogel (CA), microporous-activated carbon (AC), and different combinations of the two were evaluated for capacitive deionization application. Composite electrodes with CA and AC in the ratio of 75:25 provided the highest specific capacitance value (90 F/g at scan rate of 2 mV/s). Further, it was observed that on increasing the scan rates to up to 10 mV/s, the reduction in specific capacitance values for the electrodes with 75:25 CA/AC composition was only 5%, whereas the reduction for pure CA and pure AC electrodes were 23 and 52%, respectively. The test cell made using 75:25 CA/AC composite electrodes (size 10 cm × 10 cm with material loading of 15 mg/cm^2) showed fast adsorption and desorption cycle of ~15 min and salt removal efficiency of 51% was obtained.

Keywords: Carbon aerogel; Activated carbon; Cyclic voltammetry; Capacitive deionization

1. Introduction

Scarcity of potable water is a global problem and is getting further aggravated because of the increase in population and industrial development. Since the presently used water desalination and purification technologies such as reverse osmosis [1], electrodialysis [2], and evaporation [3] are energy intensive and expensive, there is interest in development of more efficient techniques. Capacitive deionization (CDI) which involves separation of ions by electrochemical process is receiving considerable interest as it offers advantages of low-voltage requirement, ambient operational conditions, and easy regeneration [4,5]. In the CDI process, the saline liquid is passed between two high-capacity electrodes. In the presence of electric potential, strong electrical double layers formed at the electrodes, hold the salt ions thus removing them from the saline liquid. On removal of the electric field, ions are released back to the bulk solution. This offers a simple, environmental friendly, and chemical-free regeneration.

CDI electrode should have high accessible surface area for ionic accumulation, good electrical conductivity for effective charge holding, and suitable pore size with cross-linked structure for free ionic motion. Several carbon materials such as activated carbon (AC) [6,7], carbon nanotubes (CNT) [8], and carbon aerogels (CA) [9] have been studied as CDI electrode material. AC powder offers the advantage of low cost and high surface area material but due to the presence of micropores of sizes <2 nm, the accessible surface area is low [10]. Carbon nanotubes have high surface area but suffer from high production cost and low capacity due to poor wettability [11,12]. CAs offer the advantage of high electrical conductivity and due to the presence of mesopores, provide more favorable and quicker pathways for ions to

---

*Corresponding author.

penetrate the pores and demonstrate good electrode characteristics [13]. However, being dominated by mesopores the available surface area for CA is lower than that available with AC [14] and it is also more costly as compared to AC. Due to their complimentary surface characteristics it appears that a combination of CA and AC may prove to be a more suitable electrode material as compared to pure CA and AC. With this objective, we have synthesized electrodes using different ratio of CA and AC and compared their characteristics with electrodes of pure CA and pure AC. We have investigated all electrodes for their morphology using scanning electron microscopy and for specific capacitance using cyclic voltammetry. The results obtained show that composite electrodes with CA and AC in the ratio of 75:25 provided the highest specific capacitance values and also show significantly lower reduction in capacitance with an increase in scan rate.

2. Materials and methods

2.1. CA preparation

Resorcinol (>99%, Merck) and furfural (99%, Qualigens) were dissolved in isopropanol ($\geqslant$99%, Merck) in 1:2 M ratio. The gel formulation was made using 0.38 M resorcinol and 0.76 M furfural with solid mass content of 11.5%. The gelation was carried out at a constant temperature of 60°C for 48 h. The gel was subjected to supercritical drying of isopropanol (236°C and 670 psi) in an autoclave. The dried aerogel thus obtained was carbonized in muffle furnace at 850°C under argon atmosphere to obtain mesoporous CA.

2.2. Electrode preparation

Pure CA, AC (SD fine chemicals, product code: 43,032), and their mixture in the ratio of 85:15, 75:25, 60:40, and 50:50 were used to prepare the electrodes. Polyvinylidene fluoride (PVDF) dissolved in N-methyl-2-pyrrolidone (NMP) in weight ratio of 1:18 was used as binder solution. Carbon powders and binder in the ratio 3:1 by weight was coated uniformly on the graphite sheet. The coated electrodes were immersed in water for 24 h for NMP solvent exchange. Electrodes of size 10 cm × 10 cm with active material loading of $\sim$15 mg/cm^2 were prepared for salt removal experiments. Same process was used to prepare electrode for cyclic voltammetry.

2.3. Scanning electron microscopy

Scanning electron microscopy (SEM) of pure PVDF film and different electrodes was carried out using Philips XL30CP system to study their morphology. The micrographs of these samples were recorded at a magnification of 2,000–2,500 to image the network of electrodes.

2.4. Surface area analysis

Micromeritics ASAP2020 system was used to measure surface area and pore size distribution of CA and AC samples using N_2 adsorption–desorption isotherms. The system makes use of Brunauer–Emmett–Teller (BET) theory for determining specific surface area using adsorption data and Barrett–Johner–Halendar (BJH) theory for pore size distribution using desorption data. The samples were degassed at 350°C for 15 h prior to analysis.

2.5. Measurement of capacitance

Specific capacitance of electrodes was evaluated by cyclic voltammetry measurements using AUTOLAB PGSTAT302 potentiostat in a conventional three electrode cell. The working electrode was formed with the electrode under test. Platinum electrode was used as counter electrode and a saturated calomel electrode was used as a reference electrode. Cyclic voltagrams (CV) were obtained in the potential range of −0.4 to +0.6 V in 0.5 M NaCl electrolyte. The samples were subjected to scan rates of 1, 2, 5, and 10 mV/s.

The capacitance (C) value was evaluated using following equation.

$$C = A/(\Delta V \times S) \tag{1}$$

where A is the area of the CV curve obtained by integrating the voltagram over the voltage range (ΔV) and S represents the scan rate. Test electrodes of size 1.5 cm^2, five sets for each composition, were used and their specific capacitances were evaluated.

2.6. Experiments for salt removal

Performance of electrodes was evaluated for CDI application in a desalination test cell of 100 ml capacity, a schematic of which is shown in Fig. 1. A set of two electrodes, each of size 10 cm × 10 cm were mounted in the test cell with a separation of $\sim$2.5 mm. Desalination experiments were conducted using NaCl electrolyte at a concentration of 1,000 mg/l. For adsorption cycle, potential of 1.2 V was applied to the cell and for desorption cycle the potential was reduced to 0 V. In each experiment, the effluent was continuously circulated and concentration of NaCl

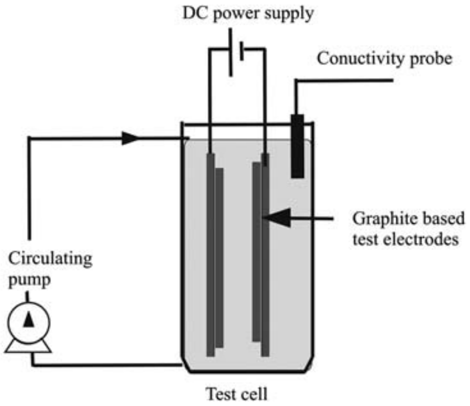

Fig. 1. Schematic diagram of the test cell used for CDI experiments.

was monitored by using conductivity meter (WTW, Cond 330i). The conductivity meter was calibrated using standard salt solutions for measuring the salt concentration. Adsorption and desorption cycles of 15 min were recorded to evaluate the salt adsorption behavior.

The NaCl salt removal was calculated according to

$$\text{Salt removal } (\%) = 100 \times (C - C_0)/C \qquad (2)$$

where C is the starting NaCl concentration and C_0 is the final NaCl concentration expressed in mg/l [15].

3. Results and discussion

3.1. Morphology of carbon electrode

SEM of pure PVDF film formed by wet exchange process is shown in Fig. 2a. The micrograph shows a regular network of pores of size 2–4 µm. These open pores of the network structure are desired as they allow fast and easy transfer of ions of electrolyte to the under layers. The micrograph of pure CA electrode formed with PVDF binder (Fig. 2b) shows that although the CA film is porous, the PVDF network is hindered resulting in restricted accessibility of under layers of CA.

In the micrograph of pure AC electrode (Fig. 2c) both the AC particles of size 5–10 µm and the PVDF network are visible. The micrograph for composite electrode of CA and AC (Fig. 2d) shows that along with the porosity of CA, the PVDF network is also visible. This suggests that addition of AC to CA helps in forming PVDF network in composite electrode. Further the composite electrode was found to have better mechanical strength than pure CA and no material loss was observed when rubbed with cloth. The coating material of the composite electrodes did not peel off with repeated use in desalination cell.

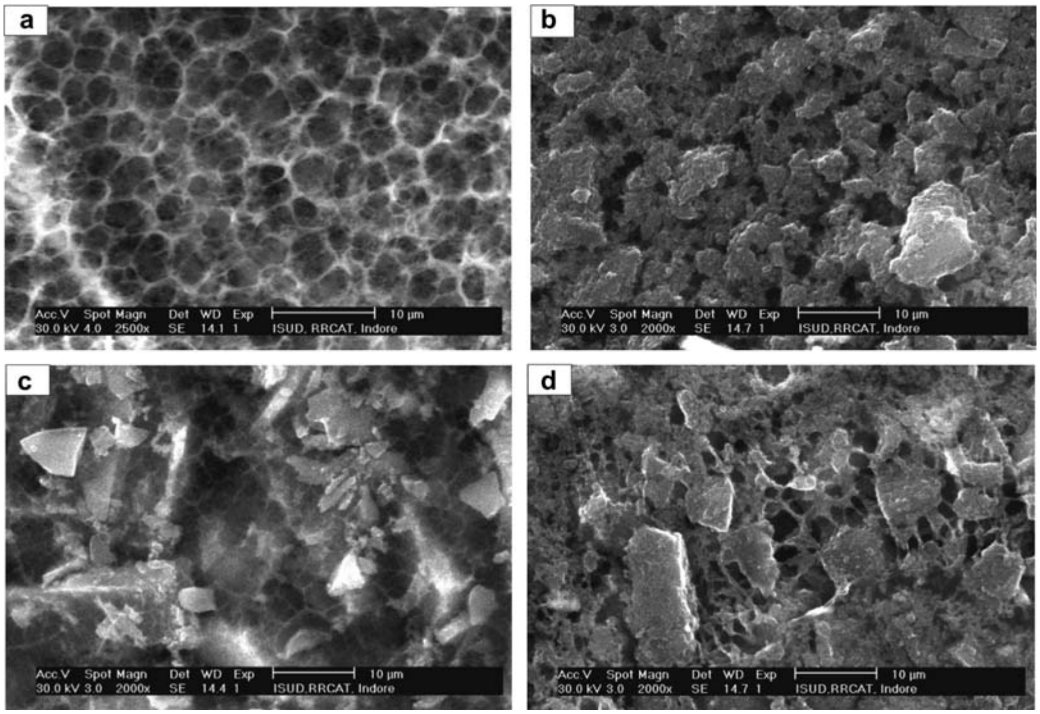

Fig. 2. SEM image of (a) pure PVDF film, (b) pure CA electrode, (c) pure AC electrode, and (d) composite electrode formed with combination of CA:AC::75:25.

Table 1
Physical properties of CA and AC powders as measured by ASAP2020

Sample	BET surface area (m^2/g)	Total pore volume (cm^3/g)	Micropore volume (cm^3/g)
CA	605	0.87	0.20
AC	1,155	0.76	0.49

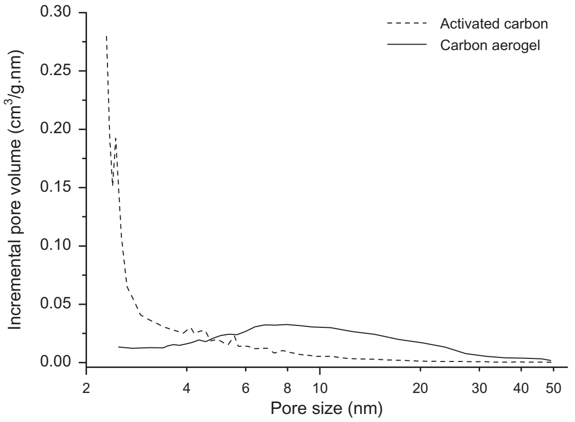

Fig. 3. Pore size distribution of CA and AC powders.

3.2. Comparison of pore size distribution

The basic physical structural parameters of AC and CA were determined using ASAP2020 and are summarized in Table 1. The pore size distribution is shown in Fig. 3. In case of CA, the maximum pore volume was in the range of pore size 3–30 nm. These mesopores of CA are favorable for fast ion transport. For AC, majority of pore volume was associated with pores of size less than 5 nm which mainly contribute to surface area.

3.3. Cyclic voltammetry

The CV of different electrodes as a function of scan rates is shown in Fig. 4. The CV of composite electrode (CA:AC::75:25) and pure CA have rectangular shape typical for an ideal double-layer capacitor [16]. This is attributed to the fact that mesoporous surfaces are readily accessible to ions. For pure AC electrode, tilted CV was obtained indicating delayed current response owing to slow transfer of ions in micropores.

The capacitance values were calculated using Eq. (1) and divided by sample weight to give specific capacitance. Specific capacitances for different types of electrodes at a scan rate of 2 mV/s are tabulated in Table 2. In case of pure CA, specific capacitance was measured to be ~80 F/g which is in agreement with other reported values for CAs [17]. The specific capacitance is significantly lower for pure AC (37 F/g) which can be attributed to absence of mesopores. AC has been used by many researchers as low-cost electrode material and the capacitance values obtained in the range of 20–40 F/g [18]. For the composite electrode with CA:AC::75:25, the specific capacitance value was the highest (90 F/g). The enhancement in specific capacitance for composite electrode can be attributed to the availability of mesopores, high surface area offered by AC and open PVDF network which allows ions to penetrate the pores. On increasing the ratio of AC to 50% in composite electrode, the capacitance value was reduced to 55 F/g.

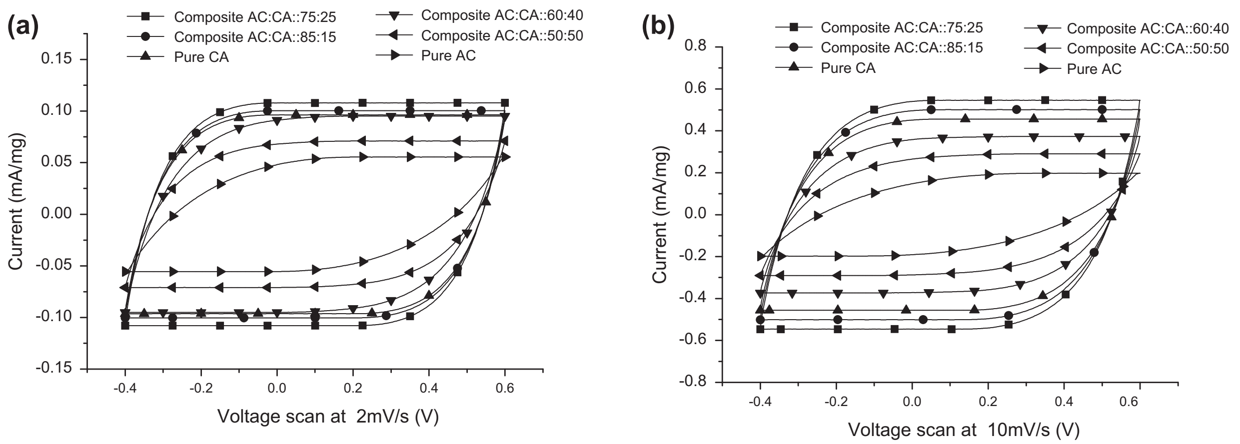

Fig. 4. Cyclic voltagrams for electrodes with pure CA, composite electrode with CA:AC::85:15, composite electrode with CA:AC::75:25, composite electrode with CA:AC::60:40, and composite electrode with CA:AC::50:50 and pure AC for (a) scan rate of 2 mV/s and (b) scan rate of 10 mV/s.

Table 2
Specific capacitance of different types of electrodes at scan rate of 2 mV/s

Electrode type	Average specific capacitance in F/g
(a) Pure CA	80 ± 4
(b) Composite of CA:AC::85:15	84 ± 4
(c) Composite of CA: AC::75:25	90 ± 4
(d) Composite of CA:AC::60:40	75 ± 4
(e) Composite of CA:AC::50:50	55 ± 4
(f) Pure AC	37 ± 3

In Fig. 5, we show the measured variation in specific capacitance as a function of the scan rate. The specific capacitance decreases with increasing scan rates. The reduction in capacitance for pure AC and pure CA with an increase in scan rate from 1 to 10 mV/s was 52 and 23%, respectively. This is consistent with the fact that while at low scan rates both micropores and mesopores are accessible to ions, at high scan rates the ions are not able to access the micropores and only small portion of total surface area is utilized. For composite electrode (CA:AC::75:25) the decrease in capacitance was significantly lower (only 5%). This is because of availability of mesopores in CA and the well-developed PVDF network which allows easy transport of ions and utilization of micropores even at higher scan rates. The observed high capacitance at fast scan rate helps in fast regeneration which is desirable for CDI applications.

3.4. CDI experiment

The capacitive deionization experiments were conducted to evaluate salt removal and their regeneration behavior [19].

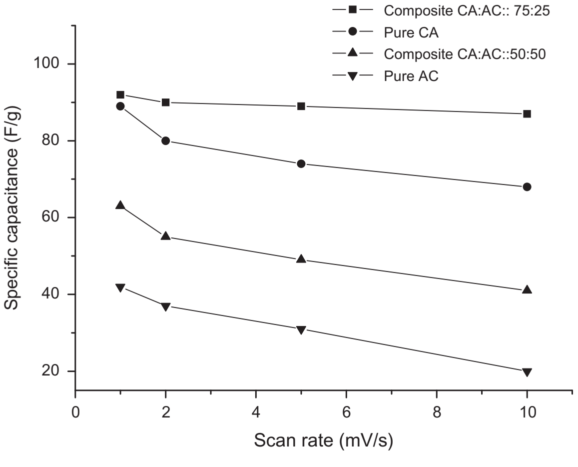

Fig. 5. Variation of specific capacitance with scan rate for different electrodes.

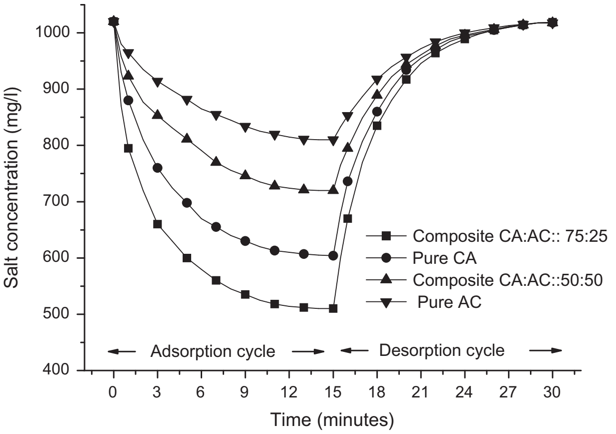

Fig. 6. Variation of salt concentration during adsorption and desorption cycle for different electrodes.

The change in salt concentration during the adsorption and desorption cycle was recorded for all the electrodes and is plotted in Fig. 6. Highest salt removal of ~51% was observed for the composite electrode with CA:AC::75:25. For the electrodes with pure CA, CA:AC::50:50 and pure AC, the salt removal obtained was 40, 29, and 20%, respectively. The equivalent salt adsorption obtained in case of composite electrode (CA:AC::75:25) was 17 mg per gram of electrode material. The corresponding salt adsorption for the electrodes with pure CA, CA:AC::50:50 and pure AC was 13 mg, 10 mg, and 7 mg, respectively.

The regeneration of the composite electrode with CA:AC::75:25 was evaluated for number of adsorption and desorption cycles in the same cell at an initial NaCl concentration of 1,000 mg/l. The variation of salt concentration is shown in Fig. 7. The regeneration efficiency of ~92% was obtained. This high regeneration

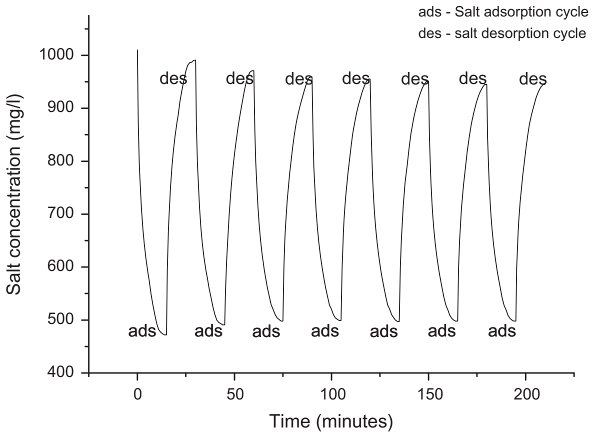

Fig. 7. Regeneration behavior of the composite electrode for repeated cycles.

efficiency is mainly attributed to free transport of ions due to presence of open network.

4. Conclusion

Studies carried out on electrodes, which synthesized using mesoporous CA, microporous-AC, and different combinations of the two showed that composite electrodes with CA and AC in the ratio of 75:25 provided the highest specific capacitance value (90 F/g at scan rate of 2 mV/s). The test cell made using 75:25 CA/AC composite electrodes (size 10 cm × 10 cm with material loading of 15 mg/cm^2) showed fast adsorption and desorption cycle of ~15 min and salt removal efficiency of 51% was obtained with regeneration efficiency of 92%. The excellent electrosorption performance of composite electrodes is ascribed to mesopores available in CA, high surface area of AC, and well-developed PVDF network. The composite electrode had good integrity and mechanical strength. Results of the studies suggest that the composite electrode with optimized composition can be suitably applied to CDI applications.

Acknowledgment

We would like to thank Shri Gopal Mohod for his help at various stages to carry out desalination experiments.

References

[1] V.G. Gude, Energy consumption and recovery in reverse osmosis, Desalin. Water Treat. 36 (2011) 239–260.

[2] L.J. Banasiak, T.W. Kruttschnitt, A.I. Schäfer, Desalination using electrodialysis as a function of voltage and salt concentration, Desalination 205 (1–3) (2007) 38–46.

[3] A.J. Morton, I.K. Callister, N.M. Wade, Environmental impacts of seawater distillation and reverse osmosis processes, Desalination 108 (1996) 1–10.

[4] T.J. Welgemoed, C.F. Schutte, Capacitive deionization technology: an alternative desalination solution, Desalination 183 (2005) 327–340.

[5] Y. Oren, Capacitive deionization (CDI) for desalination and water treatment: past, present and future (a review), Desalination 228 (2008) 10–29.

[6] L. Zou, G. Morris, D. Qi, Using activated carbon electrode in electrosorptive deionization of brackish water, Desalination 225 (2008) 329–340.

[7] J.H. Choi, Fabrication of a carbon electrode using activated carbon powder and application to the capacitive deionization process, Sep. Purif. Technol. 70 (2010) 362–366.

[8] C. Nie, Y. Zhan, L. Pan, H. Li, Z. Sun, Electrosorption of different cations and anions with membrane capacitive deionization based on carbon nanotube/nanofiber electrodes and ion-exchange membranes, Desalin. Water Treat. 30 (2011) 266–271.

[9] H.H. Jung, S.W. Hwang, S.H. Hyun, K.H. Lee, G.T. Kim, Capacitive deionization characteristics of nanostructured carbon aerogel electrodes synthesized via ambient drying, Desalination 216 (2007) 377–385.

[10] A.B. Fuertes, G. Lota, T.A. Centeno, E. Frackowiak, Templated mesoporous carbons for supercapacitor application, Electrochim. Acta, 50 (2005) 2799–2805.

[11] H.I. Kim, H.J. Kim, M. Morita, S.G. Park, Preparation and electrochemical performance of CNT electrode with deposited titanium dioxide for electrochemical capacitor, Bull. Kor. Chem. Soc. 31–2 (2010) 423–428.

[12] L.M. Chang, X.Y. Duan, W. Liu, Preparation and electrosorption desalination performance of activated carbon electrode with titania, Desalination 270 (2011) 285–290.

[13] P. Xu, J.E. Drewes, D. Heil, G. Wang, Treatment of brackish produced water using carbon aerogel-based capacitive deionization technology, Water Res. 42 (2008) 2605–2617.

[14] W. Bell, S. Dietz, United States Patent, 6297293, 2001.

[15] H. Li, Y. Gao, L. Pan, Y. Zhang, Y. Chen, Z. Sun, Electrosorptive desalination by carbon nanotubes and nanofibres electrodes and ion-exchange membranes, Water Res. 42 (2008) 4923–4928.

[16] E. Frackowiak, F. Beguin, Carbon materials for the electrochemical storage of energy in capacitors, Carbon 39 (2001) 937–950.

[17] Y.J. Lee, J.C. Jung, J. Yi, S.H. Baeck, J.R. Yoon, I.K. Song, Preparation of carbon aerogel in ambient conditions for electrical double-layer capacitor, Curr. Appl. Phys. 10 (2010) 682–686.

[18] J.B. Lee, K.K. Park, S.W. Yoon, P.Y. Park, K.I. Park, C.W. Lee, Desalination performance of a carbon-based composite electrode, Desalination 237 (2009) 155–161.

[19] M. Haro, G. Rasines, C. Macias, C.O. Ania, Stability of a carbon gel electrode when used for the electro-assisted removal of ions from brackish water, Carbon 49 (2011) 3723–3730.